# Comparative assessment of measured and modelled aircraft noise around Amsterdam Airport Schiphol

Simons, Dick G.; Besnea, Irina; Mohammadloo, Tannaz H.; Melkert, Joris A.; Snellen, Mirjam

**DOI**
10.1016/j.trd.2022.103216

**Publication date**
2022

**Document Version**
Final published version

**Published in**
Transportation Research Part D: Transport and Environment

**Citation (APA)**
Simons, D. G., Besnea, I., Mohammadloo, T. H., Melkert, J. A., & Snellen, M. (2022). Comparative assessment of measured and modelled aircraft noise around Amsterdam Airport Schiphol. *Transportation Research Part D: Transport and Environment*, *105*, Article 103216. https://doi.org/10.1016/j.trd.2022.103216

Transportation Research Part D 105 (2022) 103216

Contents lists available at ScienceDirect

Transportation Research Part D

journal homepage: www.elsevier.com/locate/trd

# Comparative assessment of measured and modelled aircraft noise around Amsterdam Airport Schiphol

Dick G. Simons [a], Irina Besnea [a,*], Tannaz H. Mohammadloo [a], Joris A. Melkert [b], Mirjam Snellen [a]

[a] Faculty of Aerospace Engineering, Section Aircraft Noise and Climate Effects, Delft University of Technology, The Netherlands
[b] Faculty of Aerospace Engineering, Section Flight Performance and Propulsion, Delft University of Technology, The Netherlands

ARTICLE INFO

*Keywords:*
Airport environmental footprint
Airport noise monitoring
Day–evening–night average level ($L_{den}$)
Dutch aircraft noise model (NRM)
NOMOS measurement system

ABSTRACT

The impressive growth of the aviation industry and the number of flights entail several environmental repercussions, such as increased aircraft noise emissions. With the worrying number of complaints from the communities around airports comes also the distrust in numerical models used for aircraft noise prediction. In this study, we compare the 'Dutch aircraft noise model' predictions to measured values from the NOise MOnitoring System (NOMOS) around Amsterdam Airport Schiphol between 2012 and 2018. While the model underestimates aircraft noise in 2012, the model prediction improved throughout the years. We observe a decreasing trend of measured aircraft-related $L_{den}$ values of 0.6 dB(A)/year (a total of 3.6 dB(A) over the investigation period), although the total number of flight movements increased during the observation time. We propose that a change in fleet mix, as well as the implementation of Noise Abatement Procedures at Schiphol Airport, fuelled this trend.

## 1. Introduction

With its emergence, the aviation industry has shown impressive growth numbers and has given rise to important economic benefits. This advantage, however, comes at the price of increased aviation-induced noise levels, resulting in annoyance, adverse economic effects, and health problems (Franssen et al., 2004; Hansell et al., 2013). Together with air pollution, environmental noise is considered an important threat to health in Europe (Basner and McGuire, 2018).

This concern is widely recognised and measures are taken to counteract it. Firstly, aircraft are made less noisy, for example by increasing the bypass-ratio of the turbofan engines and applying acoustic lining (Bertsch et al., 2015). Secondly, flight procedures and operations have been established that should result in a decrease in aircraft-induced noise in populated areas. Implementation of these measures is pushed and enforced through charges and regulations (Morrell and Lu, 2000; Schiphol Airport, 2021).

In the Netherlands, these regulations are implemented by imposing hard limits upon the yearly cumulative noise levels at locations and zones around airports. These noise levels are determined using so-called best-practice methods. These models are based on legal compliance requirements, such as those described in Document 29 of the ECAC, European Civil Aviation Conference, (ECAC.CEAC, 2016). With these methods, noise contours around airports can be calculated with low computational cost and limited model inputs, representing the noise impact of aircraft operations over large areas and, for example, a full year. The resulting contours are employed to check compliance with noise limits and estimate future aircraft impacts. The best-practice method used for calculating the noise contours around Schiphol is the so-called 'Dutch aircraft noise model'. Similar to the other best-practice

* Correspondence to: Office 3.13, Kluyverweg 1, 2629HS, Delft, The Netherlands.
*E-mail address:* i.besnea@tudelft.nl (I. Besnea).

https://doi.org/10.1016/j.trd.2022.103216
Received 2 July 2021; Received in revised form 14 January 2022; Accepted 7 February 2022
Available online 10 March 2022

methods, this model makes use of look-up tables. The tables containing the noise data are denoted noise-power-distance (NPD) tables, providing sound levels at predefined distances and thrust settings. A variety of metrics are known to be relevant measures of annoyance (Vieira et al., 2020). Noise annoyance can lead to lack of sleep, over-stress, and thus several health complications (Basner and McGuire, 2018; Dobruszkes and Efthymiou, 2020). However, out of these annoyance metrics, aircraft noise monitoring mainly considers the yearly-averaged day–evening–night average values ($L_{den}$).

This current practice of noise monitoring comes with model approximations and consequently deviations of the model predictions from the actual noise levels (Merino-Martínez et al., 2016b; Zellmann et al., 2017; Merino-Martínez et al., 2018). Approximations are, for example, those in modelling the aircraft as a point source, ignoring the noise directivity (ECAC.CEAC, 2016), and in the input, assuming a predefined variation of engine thrust settings along flight paths (Snellen et al., 2017). These known limitations of the current aircraft noise monitoring approach give rise to distrust in communities located close to the airports (Bewoners Aanspreekpunt Schiphol, 2021).

Therefore, it is important to compare the modelled $L_{den}$ values with those measured and assess their agreement quantitatively. Although an attractive means for measuring noise is to make use of arrays that allow for discriminating between the different noise sources on board the aircraft (Merino-Martínez et al., 2016a; Sijtsma, 2010; Siller, 2012; Simons et al., 2015), this is not needed for this research. The reason is that the best-practice models provide total aircraft noise levels only. The present research, therefore, considers the total aircraft noise levels recorded by individual microphones of the NOise MOnitoring System (NOMOS) around Amsterdam Airport Schiphol in the Netherlands.

In this paper we consider a six-year period of measurements to statistically investigate the long-term trends in $L_{den}$ and $L_{night}$ values, in contrast to year by year comparisons in corresponding predictions typically performed by airports. The scope of this paper is thus limited in such a way that we only address $L_{den}$ evolutions, also in comparison with the model, and not the related health issues.

The aim of the study is threefold:

(a) To investigate the trend in the measured $L_{den}$ and $L_{night}$ data over the period 2012–2018 per NOMOS station and averaged over all stations;
(b) To compare the measured $L_{den}$ values with those obtained by the 'Dutch aircraft noise model', i.e., the best-practice model used in the Netherlands for calculating noise exposure at Dutch airports;
(c) To investigate a possible correlation between the observed trend in the measured $L_{den}$ over the years with changes in operations and fleet composition at the airport.

For the third aim (c) we will use the certification data of the most frequently occurring aircraft types taking off and landing at Schiphol.

The paper is organised as follows. First, Section 2 presents the data and methods used for this study, including a presentation of the NOMOS measurement system, and the explanation of the $L_{den}$ and $L_{night}$ metrics. Also, Section 2 presents a brief description of the 'Dutch aircraft noise model' (NRM) including its differences with other best-practice aircraft noise models such as the Federal Aviation Authority's Integrated Noise Model (INM). Section 3 starts by illustrating the measured (yearly-averaged) $L_{den}$ and $L_{night}$ data for the period 2012–2018. The yearly trend is presented for a few NOMOS stations separately and a linear least-squares fit provides the trend in dB(A)/year (per station). The section continues with a comparison of the measured $L_{den}$ data with those calculated with the NRM. First, a local approach is taken to statistically investigate the agreement at each NOMOS station, followed by a global assessment at the level of the whole measuring system.

Next, in Section 4 an attempt is made to explain the observed overall trend in the measured $L_{den}$ for the period 2007–2019 by assuming that this is due to either actual changes in the fleet composition or noise mitigating procedures at Schiphol airport. Lastly, Section 5 summarises the results and a number of conclusions are drawn.

## 2. Data and methods

This study is based on the $L_{den}$ and $L_{night}$ data available at the website (European Aircraft Noise Services, 2021), which provides yearly-averaged $L_{den}$ values for the NOMOS measurement stations around Schiphol airport, see Fig. 1. A NOMOS station consists of a calibrated microphone mounted on a 6 to 10 m high mast, which continuously measures the sound in the environment. The NOMOS system comprises more than 40 stations, the locations of which are shown in Fig. 1. The figure also illustrates the population density per square kilometre. The central yellow-shaded area next to the runways (in purple lines) represents the capital of Amsterdam.

The data retrieved from the website (European Aircraft Noise Services, 2021) consists of the year-averaged $L_{den}$ and $L_{night}$ data for the period 2012–2018 concerning both aircraft noise events alone and total noise measured.

For the third aim (c) (see Section 1) we will use the certification data of the most frequently occurring aircraft types taking off and landing at Schiphol.

### 2.1. The $L_{den}$ metric

The $L_{den}$ metric (Crocker, 2008) for a period of one year (in units dB(A)) is given by

$$L_{den} = 10\log_{10}\left(\sum_{i=1}^{N_d} 10^{\frac{SEL_i}{10}} + \sum_{j=1}^{N_e} 10^{\frac{SEL_j+5}{10}} + \sum_{k=1}^{N_n} 10^{\frac{SEL_k+10}{10}}\right) - 75 \quad (1)$$

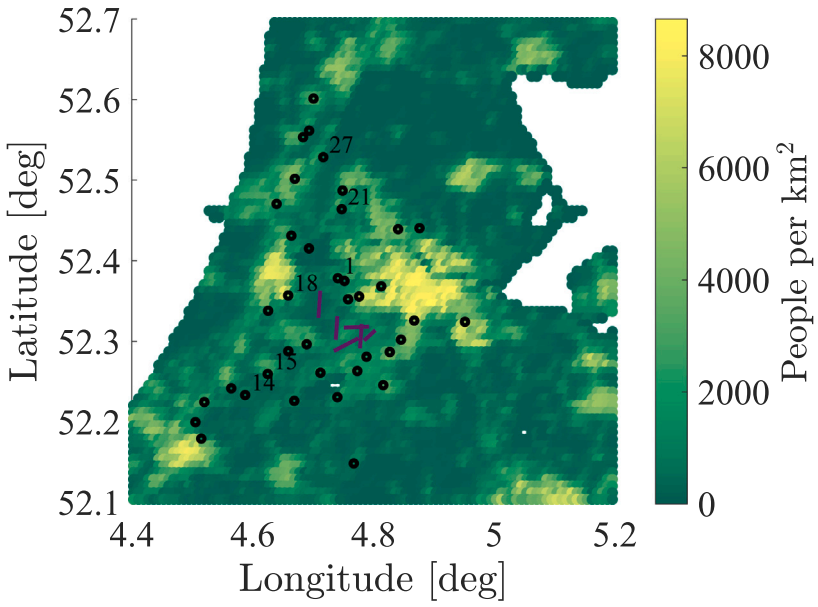


**Fig. 1.** Locations of the NOMOS stations around Schiphol Airport (black dots) (Casper.Aero, 2021). Only the IDs of the NOMOS stations described in Fig. 3 are visible. The purple lines indicate the runways of the Airport. The green/yellow background represents the population density (of 2019) around Schiphol Airport expressed in people per square kilometre (WorldPop and Center for International Earth Science Information Network (CIESIN), 2020).

**Table 1**
Noise classes per weight categories and representative aircraft.

| Weight category [ton] | Noise class 1 | Noise class 2 | Noise class 3 | Noise class 4 |
|---|---|---|---|---|
| 1 ($6 \leq$ MTOW $< 15$) | BAe-3100 Jetstream 31 | BAe-3100 Jetstream 31 | BAe-3100 Jetstream 31 | BAe-3100 Jetstream 31 |
| 2 ($15 \leq$ MTOW $< 40$) | Fokker F-28 Fellowship | Fokker F-27 Friendship | Fokker 100 | Fokker 70 |
| 3 ($40 \leq MTOW < 60$) | Boeing 737-200 | DC-90-30 ($-3$ dB)) | Boeing 737-300 HWFAP | BAe-146-200 |
| 4 ($60 \leq$ MTOW $< 100$) | Boeing 737-200 | Boeing 737-300 | Boeing 737-300 HWFAP | MD-90 |
| 5 ($100 \leq$ MTOW $< 160$) | DC-8-63 | Airbus A-310-203 ($+3$ dB) | Airbus A-310-203 | Boeing 757-200/ RB211-535E4 |
| 6 ($160 \leq$ MTOW $< 230$) | DC-8-63 | Boeing 767-300 ER ($+3$ dB) | Boeing 767-300 ER | Boeing 787-8 |
| 7 ($230 \leq$ MTOW $< 300$) | DC-10-30 ($+3$ dB) | DC-10-30 | DC-10-30 ($-3$ dB) | Boeing 777-200 |
| 8 ($300 \leq$ MTOW $< 400$) | Boeing 747-200B | Boeing 747-300 | Boeing 747-400 | Boeing 777-300ER |
| 9 (MTOW $\geq 400$) | – | – | – | Airbus |

where $N_d$, $N_e$ and $N_n$ are the number of (detected) aircraft noise events during day-time (07.00: 19.00), evening-time (19.00: 23.00) and night-time (23.00: 07.00), respectively. $SEL_i$, $SEL_j$ and $SEL_k$ are the corresponding Sound Exposure Levels of the day-time, evening-time and night-time events, respectively. The term $-75$ dB(A) originates from the normalisation for the one year period (in seconds), i.e., it is equal to $-10\log_{10}(365.25 \times 24 \times 3600)$. The Sound Exposure Level of an aircraft noise event is given by

$$SEL = 10\log_{10}\left(\int_0^T 10^{\frac{L_A(t)}{10}} dt\right) \tag{2}$$

where $L_A(t)$ is the (measured) instantaneous A-weighted sound pressure level of the event and the integration time $T$ is chosen such that it covers the time interval during which $L_A(t)$ is not more than 10 dB(A) below the maximum value of $L_A(t)$.

Typically, 30% of the population is highly annoyed by aircraft noise at $L_{den} = 55$ dB(A) (Gjestland, 2019) although large differences for different airports can occur and also non-acoustic factors such a demographic, social and personal, can influence the perceived noise annoyance. Contours in $L_{den}$ around this value are determined for airports, with a range of 40 dB(A) to 70 dB(A).

The $L_{night}$ metric (also for a period of one year and expressed in units dB(A)) is similar to $L_{den}$. According to the (Council of the European Union, 2002), $L_{night}$ is computed for the aircraft events during night-time, without applying the 10 dB(A) penalty. Hence, it is given by

$$L_{night} = 10\log_{10}\left(\sum_{k=1}^{N_n} 10^{\frac{SEL_k}{10}}\right) - 70.2 \tag{3}$$

The normalisation term of $-70.2$ dB(A) equals $-10\log_{10}(365.25 \times 8 \times 3600)$ as there are only 8 h night-time.

### 2.2. Dutch aircraft noise model (NRM)

The noise level calculations within the current Dutch best-practice model for predicting aircraft noise in the Netherlands, particularly at Schiphol Airport (van der Wal et al., 2001a,b; Heppe, 2014), comprises the following steps:

(a) A limited number of aircraft classes are specified that represent multiple aircraft types with comparable weight and noise characteristics. Aircraft are subdivided into nine weight categories based on their maximum take-off weight (MTOW), each of which is linked to four noise classes based on aircraft noise certification data. This combination results in 36 aircraft classes each having one representative aircraft, see Table 1.
Noise class 1 represents the oldest, i.e., loudest, aircraft. Newer i.e., less noisy, aircraft, are represented by higher noise classes (up to class 4). Because of this simplified classification, noise characteristics are assumed to be independent of the actual aircraft configuration and engine type. Aircraft class 4/3 (i.e., weight category 4, noise class 3), accounting for a considerable amount of flights at Schiphol (see Section 4), is represented by the Boeing 737-300 HWFAP (which stands for 'hard wall forward acoustic panel' (Geng et al., 2015)). Most of the operational Boeing 737 (including Boeing 737-800) and Airbus 320 aircraft are placed in this class.

(b) Flight profiles for each aircraft class are selected based on the chosen procedure and the distance of the flight. A flight profile table gives height, flight speed and corresponding thrust setting as a function of distance for various distance segments. Since the flight profiles are constructed for ideal situations, the actual flight profile will deviate from these, e.g., because of pilot input and actual aircraft configuration.
There are nine procedures (numbered from 00 to 08) for take-off, including standard ICAO procedures, but also airport specific procedures such as NADP (Noise Abatement Department Procedure). There are three procedures (numbered 10, 11 and 12) for landing, including the standard landing configuration ('normal instrument approach') and procedures with adjusted aircraft settings to reduce the emitted noise. For each of the nine take-off procedures there are four class numbers (numbered 00 to 03) based on the distance to destination of the flight. For each of the three landing procedures there are three class numbers (00, 01 and 09), providing additional information about the landing procedure, like initial approach height in case of 'step approach' (00 and 01) or the 'continuous descent approach' (09). For each procedure/class combination, fixed flight profiles have been determined.

(c) The noise data corresponding to a representative aircraft are listed in a Noise-Power-Distance (NPD) table consisting of the overall A-weighted sound pressure level (in dB(A)) for predetermined source-receiver distances (in m) and engine settings (in thrust force in kN or fan rotational speed in rpm). Noise levels at other distances and thrust settings than those listed in the NPD table are obtained by linear interpolation. The NPD data do not account for noise directionality, i.e., the aircraft is modelled as an omnidirectional point source. Each NPD table is assigned a unique number, for instance, 469 for the Boeing 737-300 HWFAP.

(d) The overall A-weighted sound pressure levels $L_A$ obtained from the NPD tables are corrected for the effect of lateral attenuation using simple empirical formulas. This takes into account the effect of attenuation due to the ground (assumed to be a flat sand surface covered by grass) and, to a certain extent, meteorological effects and the effect of directionality of the aircraft sound. The ground attenuation effect, however, vanishes for elevation angles larger than 20° (the elevation angle is the angle the line connecting source (the aircraft) and receiver makes with the ground). Further, the effect of directionality is maximally 3 dB(A).

(e) A grid on the ground is defined around the flight path, where the $x$-coordinate is parallel to the flight path and the $y$-coordinate perpendicular to it. Given a fixed grid point $(x, y)$, the instantaneous distance and thrust setting are determined from the given flight profile as a function of time. Time is obtained using the ground velocity in the flight profile table. Typically, a time step of 1 s is chosen. Subsequently, the instantaneous $L_A$ is calculated as a function of time by linear interpolation of the data in the relevant NPD table. Then, from the obtained $L_A$ versus time curve the *SEL* value is determined using Eq. (2). This calculation procedure is repeated for each grid point defined, yielding a noise contour of the *SEL* metric for a particular flight movement.
As an example we consider a Boeing 737-300 HWFAP taking off using procedure 06 (NADP2) and take-off class number 00 (distance to destination $< 750$ km). This flight movement is denoted 4690600, a concatenation of NPD table number, flight procedure and the class number of the flight. Figs. 2(a) and 2(c) show the flight profile and the corresponding *SEL* noise contour, respectively. As a second example we consider a landing Boeing 737-300 HWFAP using procedure 10 (3° glide angle, normal instrument approach) and landing class numbers 00 (initial approach altitude 2000 ft). The results of the modelling for this flight movement 4691000 are shown in Figs. 2(b) and 2(d).

The $L_{den}$ metric is calculated per grid point using Eq. (1) taking into account all *SEL* values calculated for the various flight movements occurring during a period of one year.

Although the best-practice modelling approaches are quite similar, there are some differences between them, and thus they can yield different results. One such other best-practice model is FAA's Integrated Noise Model (INM) which is in compliance with ECAC's Document 29. Both NRM and INM make use of the NPD look-up tables. Differences between NRM and INM involve, among others, the lateral sound attenuation, as a result of which INM calculations result in a higher noise load close to the airport and a lower noise load further away from the airport (Strategische Milieuverkenning, 2008). Another difference involves part of the calculation method, as the NRM is a point-based model and the INM is a segment-based calculation model.

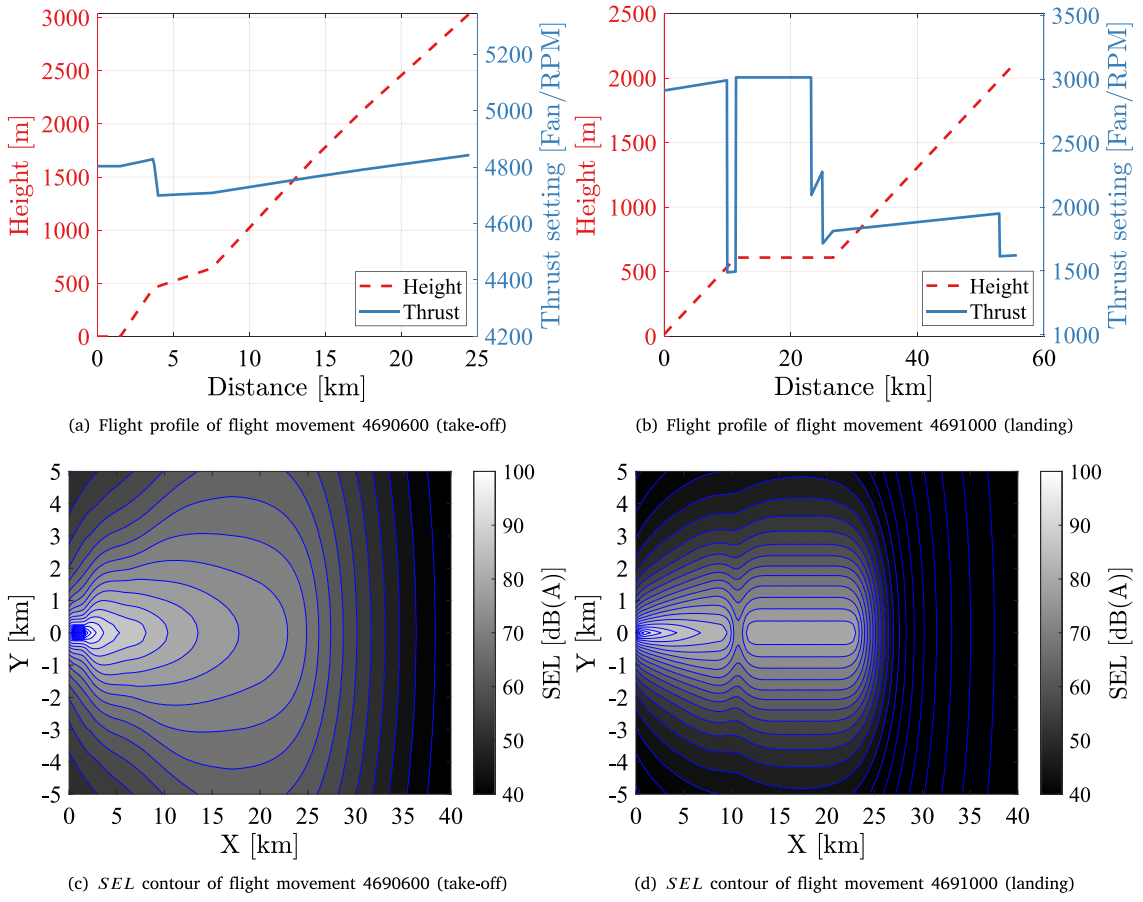


(a) Flight profile of flight movement 4690600 (take-off)

(b) Flight profile of flight movement 4691000 (landing)

(c) $SEL$ contour of flight movement 4690600 (take-off)

(d) $SEL$ contour of flight movement 4691000 (landing)

**Fig. 2.** Flight profile (a) and corresponding $SEL$ contour (c) of flight movement 4690600 (take-off). Flight profile (b) and corresponding $SEL$ contour (d) of flight movement 4691000 (landing).

## 3. Results

### 3.1. Trends in measured $L_{den}$

Measured $L_{den}$ and $L_{night}$ data over the period 2012–2018 (European Aircraft Noise Services, 2021) are shown in Fig. 3 for a few stations selected for illustrative purposes. A linear fit over time illustrates that in most cases a significant decrease is obtained. The same trend is observed in the case of other stations. Five out of 26 stations, like station 18 (see Fig. 3), show an anomalous decrease in $L_{den}$ in the year 2015 with a subsequent upward trend in the period 2016–2018. However, we did not find any correlation of this phenomenon with the location of the stations, specific use of runways, temporary closures, maintenance, etc.

Additionally, all measured $L_{den}$ and $L_{night}$ data is shown as a function of year (blue squares) in Fig. 4, both for the aircraft noise events and the total measured noise. The data per year are averaged over all NOMOS stations (thick red line). Subsequently, these averaged data are linearly fitted (dashed red line). For the aircraft noise events (Figs. 4(a) and 4(b)) an overall decrease of 3.6 dB(A) and 3.1 dB(A) over the 6-year period is obtained for $L_{den}$ and $L_{night}$, respectively, which corresponds to a 0.6 dB(A)/year decrease.

For the total noise (Figs. 4(c) and 4(d)) there is a slight $L_{den}$ increase of 0.03 dB(A)/year and a strong $L_{night}$ decrease of 0.45 dB(A)/year. This may show that a lot of the night-time noise was mainly due to aircraft-related events and with its decrease, the total noise during night-time also decreases. The decrease of night-time aircraft noise may be attributed to the implementation of Continuous Descent Approaches (CDA), although this only holds for stations at a sufficient distance from the runway (> 10 km). In addition, the increased airport charges for take-off and landing that Schiphol airport has imposed and the change in fleet composition can play important roles in this respect (see Section 4).

Although the original data may look fairly scattered, these trend values are statistically significant, as demonstrated later. A 3 dB(A) decrease in $L_{den}$ for aircraft noise corresponds to a reduction of a factor of two in number of flight movements, provided the aircraft in the fleet are the same (i.e., they have the same loudness). Hence, a decrease of 3.6 dB(A) (in 6 years) is substantial.

Further note that, on average, the $L_{den}$ for total noise is 10 dB(A) higher than the noise due to aircraft events alone, i.e., the contribution of background noise to the $L_{den}$ for total noise (background plus aircraft events) is dominant. The $L_{den}$ for total noise

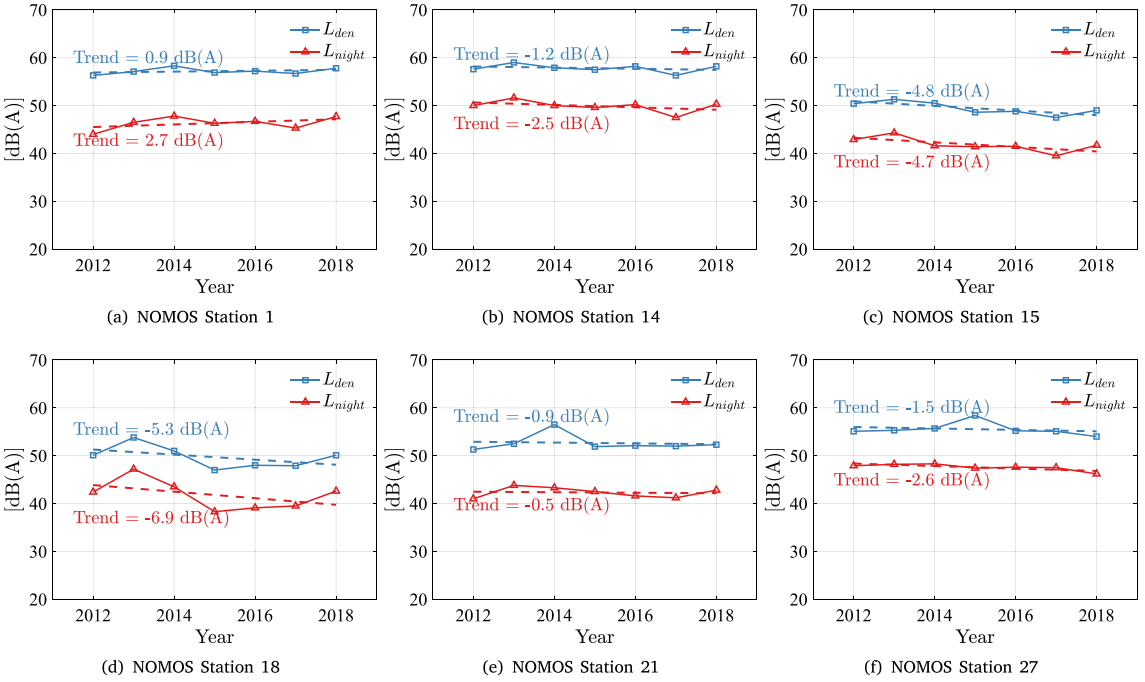


(a) NOMOS Station 1 (b) NOMOS Station 14 (c) NOMOS Station 15

(d) NOMOS Station 18 (e) NOMOS Station 21 (f) NOMOS Station 27

**Fig. 3.** Measured $L_{den}$ and $L_{night}$ as a function of year for six selected NOMOS stations (only aircraft noise events). Both the $L_{den}$ and $L_{night}$ data are linearly fitted to quantify the trend in dB(A) over 6 years as indicated.

amounts to approximately 65 dB(A) (see Fig. 4(c)). This can be explained by a constant and continuously present A-weighted sound pressure level of 58 dB(A) due to background noise. Such an average background noise level is considered realistic. The $L_{den}$ for aircraft noise events alone amounts to approximately 55 dB(A), which corresponds to 30 events per hour during day-time, each event having a *SEL* value of about 80 dB(A) (which is a realistic value for aircraft events).

Fig. 5 shows the $L_{den}$ levels for all stations, identified by their ID, for 2012 and 2018. As concluded from the previous figures as well, we notice an overall decrease in $L_{den}$ of about 3 dB(A) from 2012 to 2018. For the stations active in both years (stations 1 to 32 and 92) there are no clear 'winners' (i.e. decrease of $L_{den}$) or 'losers' (i.e. increase of $L_{den}$). Extreme outliers, such as NOMOS 30 may have been subjected to maintenance or calibrations.

### 3.2. Comparison with modelled $L_{den}$ data

To create a more complete overview of the yearly noise trend at Schiphol, we consider the 'Dutch aircraft noise model' (NRM) used for calculating the noise contours around Schiphol. We compare the model with the measured values in order to identify patterns in the trends. This section is divided into a local and global assessment of the agreement between measurements and model.

#### 3.2.1. Local agreement

For a local investigation, the differences between modelled and measured $L_{den}$ values throughout an entire year were analysed, see Fig. 6 where NOMOS stations are plotted in blue squares. The mean difference is marked with a dashed red horizontal line surrounded by its 68% confidence interval (mean ±standard deviation). Shown with the solid black line is the zero difference between the measured and modelled values. It can be observed that in 2012 the model underestimates the measured $L_{den}$ ($\bar{L}_{den}^{meas} > \bar{L}_{den}^{mod}$). For 2018 the opposite is true, where the distribution is also more peaked and closer to zero. One should notice the different number of active stations in different years.

The correlation coefficient between the absolute difference (between modelled and measured values) was studied with respect to the distance to each NOMOS station's closest runway. Table 2 presents the correlation coefficient and associated $p$-value.

We consider, in line with common practice in statistical analysis, a $p$-value below 0.05 (5% error probability) as statistically significant. Given that all $p$-values are above the significance level $\alpha = 0.05$, we cannot conclude that there is a correlation between the distance to the closest runway and the absolute difference between the measurements and modelled values. Given the lower correlation coefficient values, this is even more so the case for later years.

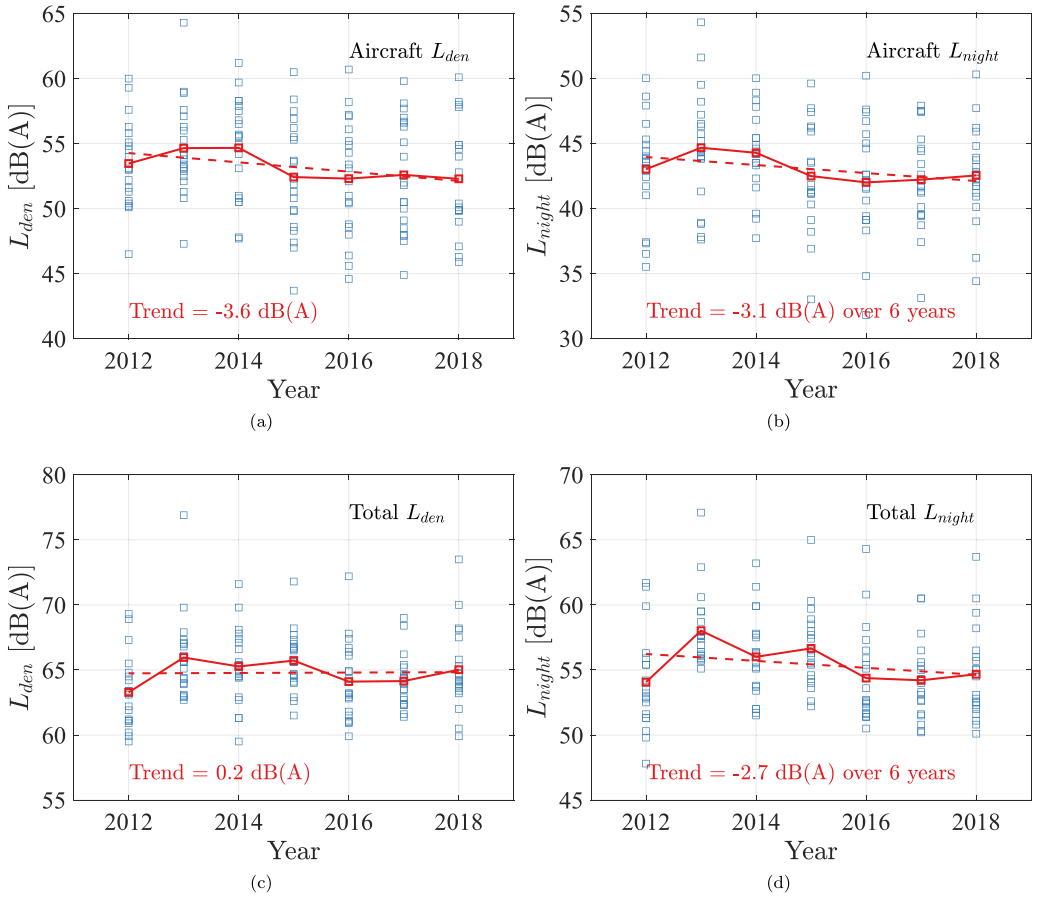


**Fig. 4.** All measured $L_{den}$ and $L_{night}$ data versus year (blue squares) for the aircraft noise events alone, (a) and (b), and the total measured noise, (c) and (d). For each year, the data have been averaged over all stations (red solid line) and subsequently fitted by a linear function (red dashed line). The obtained trends are indicated in the figures. (For interpretation of the references to colour in this figure legend, the reader is referred to the web version of this article.)

**Table 2**
Correlation coefficients between the absolute difference (between measured and modelled $L_{den}$ values) and the distance to the closest runway.

| Year | $\rho$ | $p$-value |
|---|---|---|
| 2012 | −0.30 | 0.16 |
| 2013 | −0.37 | 0.07 |
| 2014 | −0.27 | 0.19 |
| 2015 | −0.29 | 0.16 |
| 2016 | −0.16 | 0.36 |
| 2017 | −0.10 | 0.53 |
| 2018 | −0.08 | 0.60 |

### *3.2.2. Global agreement*

In this section we investigate the global agreement between measured and modelled $L_{den}$ values. Fig. 7 shows maps of the modelled $L_{den}$ data for the Schiphol area (aircraft events only) for the years 2012 and 2018. These maps of size 54 km × 67 km have been calculated using the 'Dutch aircraft noise model'. The measured $L_{den}$ values at the NOMOS station positions have been superimposed on the maps. The illustration allows a visual inspection of how well the measurements agree with the model. The thin white lines give a rough indication of the Dutch coastlines. There are not many differences between the modelled values of these two years. What can be observed is that some tracks are more pronounced in 2012 compared to 2018 at a level of around 50 dB(A). This suggests that in the later years, the lateral dispersion of the tracks has been taken into consideration.

For a more quantitative comparison, scatter diagrams of measured $L_{den}$ values against modelled $L_{den}$ values are exemplary shown in Fig. 8 for the years 2012 and 2018. Only the modelled $L_{den}$ values for the NOMOS station positions are considered now. The

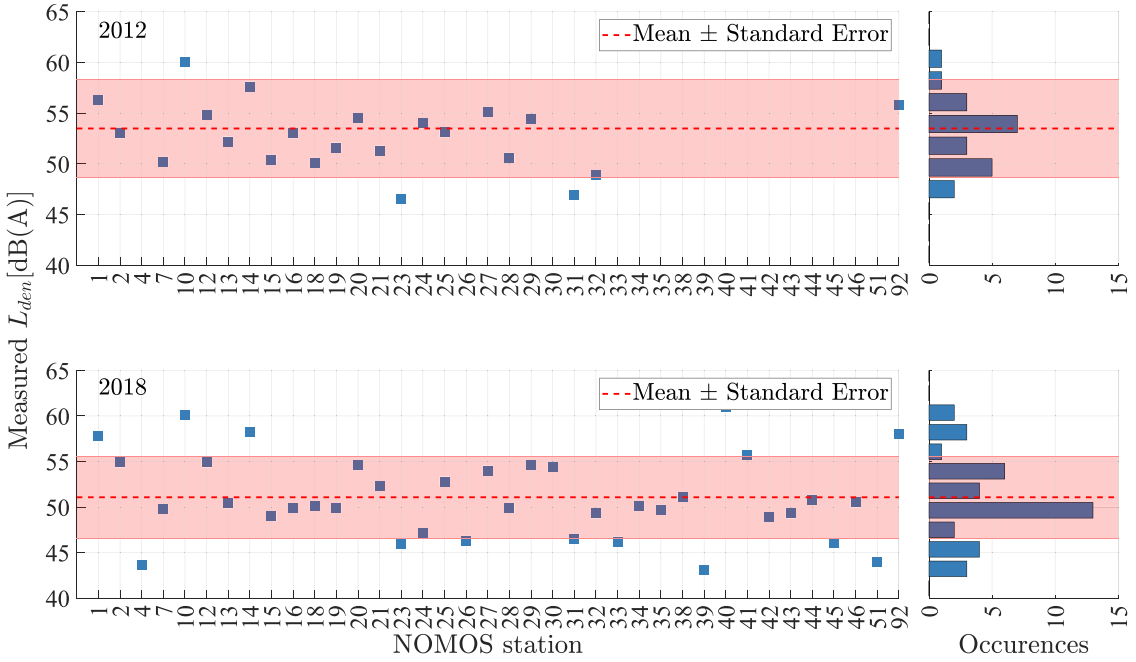


**Fig. 5.** Distribution of measured $L_{den}$ data per NOMOS station for the years 2012 (top) and 2018 (bottom). The plots contain a scatter plot of all NOMOS stations (blue squares), and a distribution of these measured $L_{den}$ with the mean as a dashed red line and the spread in red background.

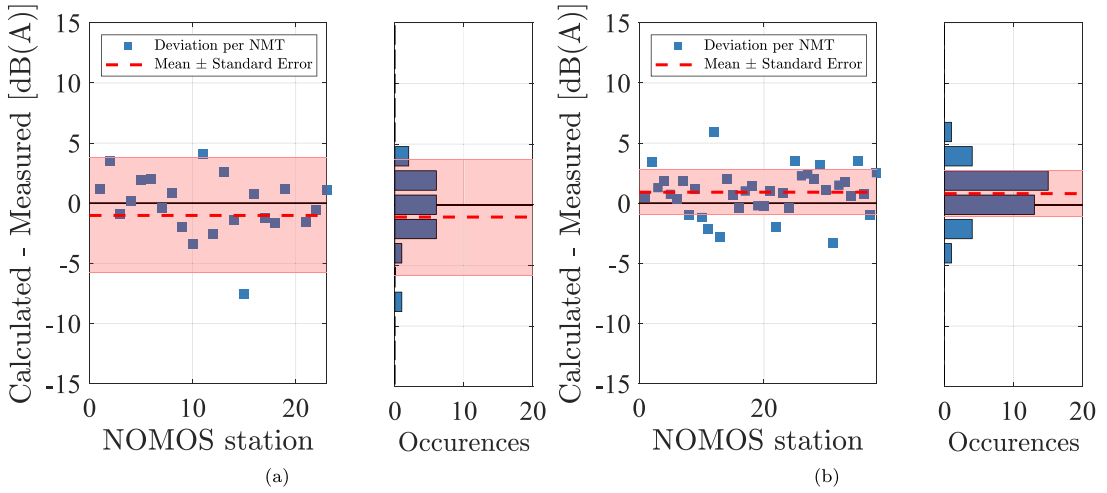


**Fig. 6.** Distribution of deviation between modelled and measured $L_{den}$ data per NOMOS station for the years 2012 (a) and 2018 (b). The plots contain a scatter plot of all NOMOS stations (blue squares), and a distribution of this deviation with the mean as a dashed red line, zero deviation as a solid black line, and the spread as red background.

correlation coefficient $\rho$ is indicated in the figures. From Fig. 8, the same observation as in Fig. 6 can be made, i.e. the modelled $L_{den}$ values for 2012 underestimate the measurements and the agreement increases in later years.

Table 3 lists the correlation coefficient $\rho$, the coefficient of determination $\rho^2$ and the corresponding $p$ -value between measured and modelled values for all years considered. Furthermore, the mean ($\mu$) and standard deviation ($\sigma$) of the quantity $L_{den}^{mod} - L_{den}^{meas}$ are used as metrics to evaluate the agreement between measurements and model.

It is observed that for the years 2015, 2016, 2017, and 2018, the agreement between measurements and model is quite good. For the years 2014, 2013 and especially 2012, the model-data agreement gets worse. All correlation coefficients obtained are statistically significant as can be observed from the $p$-values. Note that the modelled mean $L_{den}$ is virtually constant over the years. One possibility is that the increase in the number of flight movements is compensated by the less noisy aircraft. The lower measured

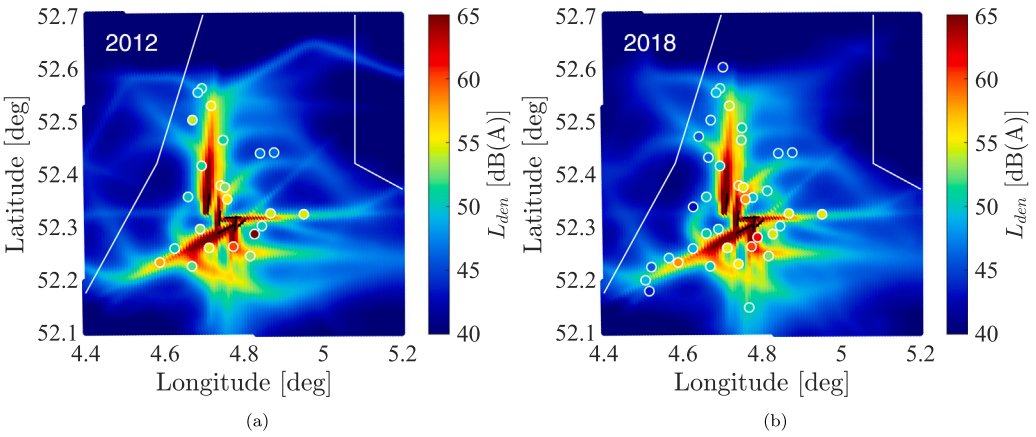


**Fig. 7.** Maps of modelled $L_{den}$ (for a grid of size 54 km × 67 km) for the years 2012 (a) and 2018 (b). Measured $L_{den}$ values at the NOMOS stations are also shown (colour inside the white circles). The Dutch coastlines are indicated with white lines. The Schiphol runways are indicated by the solid black lines. (For interpretation of the references to colour in this figure legend, the reader is referred to the web version of this article.)

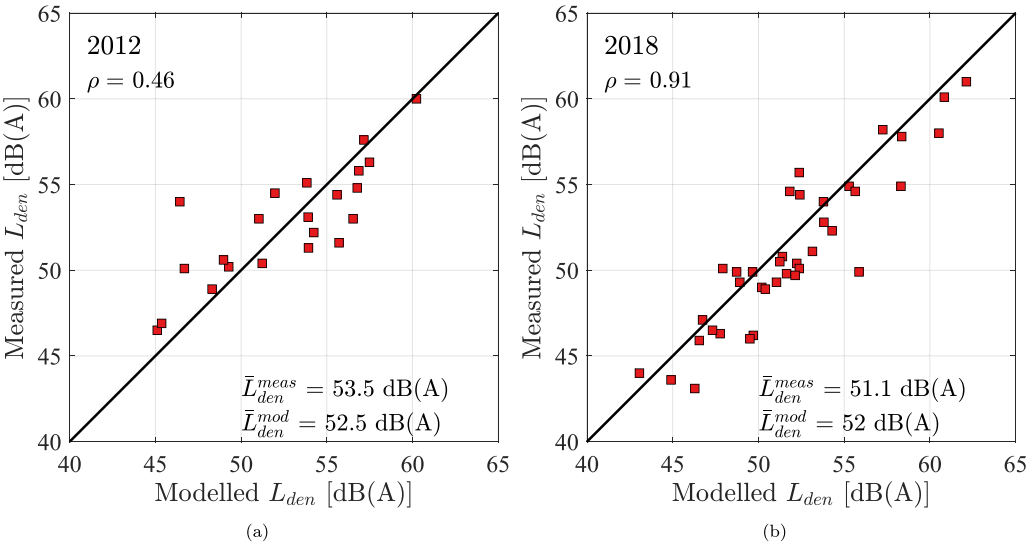


**Fig. 8.** Scatter diagrams of measured $L_{den}$ against modelled $L_{den}$ for the NOMOS station positions for the years 2012 (a) and 2018 (b). The correlation coefficient is indicated as $\rho$ in the top-left corners.

**Table 3**
Correlation coefficients between modelled and measured $L_{den}$, its variance and $p$-values, and the average difference and standard deviation for all NOMOS stations.

| Year | $\bar{L}_{den}^{meas}$ | $\bar{L}_{den}^{mod}$ | $\rho$ | $\rho^2$ | $p$-value | $\mu$ | $\sigma$ |
|---|---|---|---|---|---|---|---|
| 2012 | 53.5 | 52.5 | 0.46 | 0.21 | $2.8 \times 10^{-2}$ | −1.0 | 4.8 |
| 2013 | 53.9 | 52.3 | 0.72 | 0.52 | $1.1 \times 10^{-4}$ | −1.7 | 3.0 |
| 2014 | 54.3 | 52.4 | 0.72 | 0.52 | $7.2 \times 10^{-5}$ | −1.9 | 3.2 |
| 2015 | 51.7 | 52.1 | 0.89 | 0.80 | $2.1 \times 10^{-9}$ | 0.3 | 2.1 |
| 2016 | 51.3 | 52.2 | 0.92 | 0.85 | $3.3 \times 10^{-14}$ | 0.9 | 1.9 |
| 2017 | 51.1 | 52.0 | 0.91 | 0.83 | $2.7 \times 10^{-15}$ | 0.9 | 2.0 |
| 2018 | 51.1 | 52.0 | 0.91 | 0.83 | $1.5 \times 10^{-15}$ | 0.9 | 1.9 |

$L_{den}$ values in 2015 might be due to the effects of the updated Noise Abatement Departure Procedures (NADP-2) implemented the previous year. To a certain extent this is also seen in the modelled mean $L_{den}$. These assumptions are addressed in the next section.

We further again quantify the $p$-value as a measure for statistical significance of the observed correlations (Chatfield et al., 1987). Note that for all years, the found $p$-values are below 0.05 and thus statistically significant. The correlation coefficients for the years

2015–2018 are higher than for the period 2012–2014, thus indicating an improved agreement between measurements and model over the years.

The coefficient of determination $\rho^2$ is equal to the fraction of the variability in two variables that is shared, i.e., when $\rho^2$ is above 0.80, as is the case for the years 2015–2018, more than 80% of the total variability observed in measured $L_{den}$ is explained by variations in modelled $L_{den}$. $\rho^2$ is smaller for the years 2012–2014 than for 2015–2018, where also the $p$-value is higher, especially for the year 2012.

The metric $\sigma$ is a measure for the spread of the scatter diagram of measured $L_{den}$ against modelled $L_{den}$ and this metric considerably decreases from 2012 to 2018. At the same time, the metric $\mu$, i.e., the mean difference between measured $L_{den}$ and modelled $L_{den}$, is less than 1 dB(A) in absolute value, except for the years 2013 and 2014. However, $\mu$ changes from sign negative to positive, i.e., for the years 2015–2018 the measured $L_{den}$ is, on the average, lower than the modelled $L_{den}$, whereas for the years 2012–2014 the reverse is true (as concluded earlier). The modelled $L_{den}$ is fairly stable over the period 2012–2018. Hence, the jump in $\mu$ from 2014 to 2015 is mainly due to the measured mean $L_{den}$.

In conclusion, the model-data agreement in the period 2015–2018 is quite good on the average ($\mu$ is less than 1 dB(A)). The remaining scatter in the differences, as reflected by $\sigma$ (2 dB(A) for the same period), is mostly due to assumptions in the model concerning adopted thrust values and assumed standard flown trajectories (see Section 2.2).

## 4. Discussion

In this section we discuss the observed trend in the measured $L_{den}$ data, see Section 2.1. We postulate that the average decrease of −3.6 dB(A) over the period 2012–2018 (i.e., a decrease of −0.6 dB(A)/year) is due a to various factors, such as the implementation of noise abatement procedures and changes in fleet composition at Schiphol Airport.

Noise abatement measures implemented at Schiphol Airport include runway usage (in such a way to avoid flying above residential areas), Noise Abatement Departure Procedures (NAPD-2), Continuous Descent Approaches (CDA) during nighttime, higher take-off and landing rates for noisy aircraft, and higher rates for movements during nighttime (Schiphol Airport, 2021). By default, certain runways are assigned for either take-off or landing. However, due to the instability in wind directionality, the use of runways is changed regularly to provide safer operations. Fig. 9(a) shows the measured $L_{den}$ and the corresponding population density at each NOMOS location for both 2012 and 2018. We noticed that the stations situated in the more populated areas yielded similar results for both years in most cases. Fig. 9(b) shows the flown trajectories for July 2018 at Schiphol Airport. The superposition on the population density illustrates how the procedures are meant to avoid the residential areas and cities.

In addition to this, according to the State Decree of May 2014 (Ministerie van Infrastructuur en Milieu, 2014), Schiphol Airport enforced NADP-2 for departure procedures. This procedure aims at reducing noise in areas further away from Schiphol airport by starting its climb earlier and at a lower altitude than the previously used NADP-1 take-off (Veerbeek and Brouwer, 2012). Its implementation in 2014 might explain the sudden decrease of $L_{den}$ values between 2014 and 2015 (see Fig. 4(a) and Table 3).

Another factor that must be taken into account is the change in fleet mix at Schiphol Airport. The total number of flight movements per year is shown in Fig. 10 for the period 2007–2019. This data includes freight flights, however, these are limited to 20,000 per year. We select this new time window as it includes the period over which the aircraft noise was investigated, but also the years 2007 and 2019 for which certification data was available.

It is observed that the number of flights has increased from 440,000 around 2007 to 500,000 around 2019. This has the limited effect of about $10\log_{10}(5/4.4) \approx 0.55$ dB(A) increase in $L_{den}$ in this 12 year period, i.e., an increase of approximately 0.04 dB(A)/year. Zooming in on the time segment 2012–2018, we observe the same trend of 0.04 dB(A) increase per year. Hence, the observed decrease in $L_{den}$ of 3.6 dB(A)/year over the same period can be explained, at least partly, by the occurrence of less noisy aircraft in 2018 compared to those in 2012. To evaluate this hypothesis, the number of flight movements per year for the most frequently occurring aircraft types at Schiphol are shown in Fig. 11 for the period 2007–2019.

From Fig. 11 the following observations can be made:

(1) a transition of Boeing 737-300 and 737-400 flights in 2007 to mainly Boeing 737-700 and 737-800 flights in 2019 (Fig. 11(a));
(2) an increase in Airbus 319, 320, 321 flights from 60,000 in 2007 to 100,000 in 2019 (Fig. 11(b));
(3) a transition of Fokker 50, 70 and 100 flights in 2007 to mainly Embraer 170 and 190 flights in 2019 (Fig. 11(c));
(4) a decrease of Boeing 747-400 and 767 flights in the period 2007–2019 and an increase of Boeing 777 and 787 flights in the same period (Fig. 11(d)).

To investigate whether there are less noisy aircraft in 2019 compared to 2007, we consider the noise certification data (EASA, 2020) of the most frequently occurring aircraft types at Schiphol. These data are given in Table 4 where the left 5 columns of the table are representative for the situation in 2007 (mostly Boeing 737-300, 737-400, 737-500, Boeing 767-300, Boeing 747-400 and Fokker 70 and 100) and the right 5 columns are representative for the situation in 2019 (mostly Boeing 737-700, 737-800, Boeing 777-200, 777-300, Boeing 787-9, Embraer 170 and 190 and Airbus 319, 320, 321). Also given in Table 4 are the MTOW values of the various aircraft. Noise certification data are provided at three positions relative to the flight path and are expressed in the unit EPNdB (effective perceived noise level, a noise metric similar to *SEL*). These positions are denoted ‘lateral’, ‘flyover’ and ‘approach’.

The certification data are graphically depicted in Fig. 12, where we have plotted the EPNdB values as a function of MTOW. The blue squares are the noise certification data for the situation of 2007, whereas the red squares are the data for the situation of 2019. The data have been linearly least-squares fitted in order to be able to assess underlying trends.

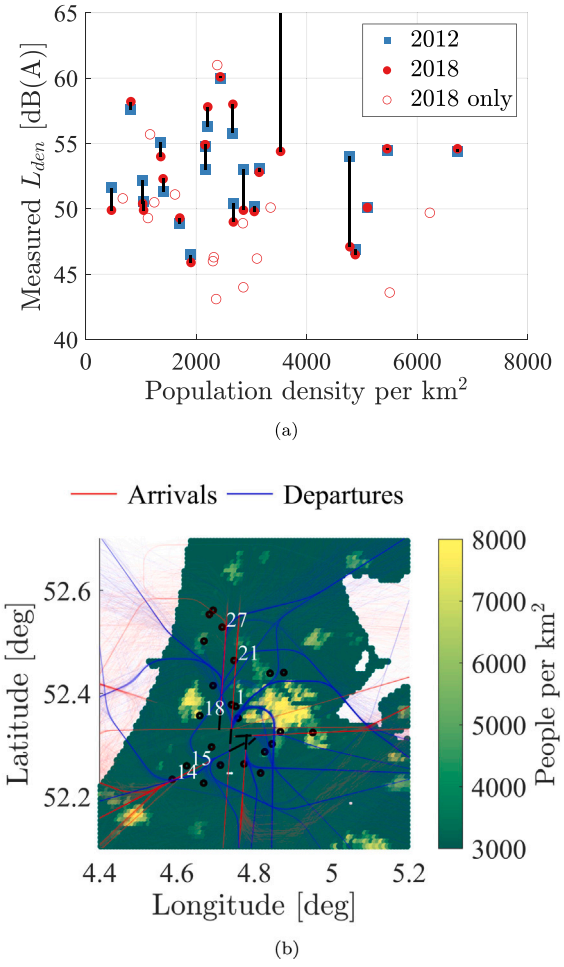


**Fig. 9.** (a) The measured $L_{den}$ for all NOMOS stations of 2012 (blue squares) and 2018 (red circles) against the population density from 2019 at their location. 2018 stations active since 2012 are marked with filled red circles and they are connected to their 2012 correspondent with a solid black line. One outlier of 2012 was excluded from this figure. (b) Operations at Schiphol Airport of July 2018. The green/yellow background represents the population density map of 2019. The black short lines indicate the runways and the black dots are the locations of the NOMOS stations. The red lines show arrivals and the blue lines departures. Only the IDs of the NOMOS stations shown in Fig. 3 are visible. (For interpretation of the references to colour in this figure legend, the reader is referred to the web version of this article.)

The 'flyover' and 'approach' linear regressions of 2019 are below those of 2007, particularly at higher MTOW values. For the 'lateral' data points this is less obvious, although it is still the case for the highest MTOW values. Overall, EPNdB levels for 2019 are 1–5 EPNdB lower than for 2007 (depending on MTOW value), which indeed helps explaining the significant decrease in measured $L_{den}$ over this period.

## 5. Summary and conclusions

In this research triggered by increasing distrust and complaints of local communities around Schiphol, we have investigated the level of agreement between the NOMOS-measured $L_{den}$ values and those predicted by the 'Dutch aircraft noise model' (NRM). In this best-practice modelling approach, substantial approximations of the real world are made and hence deviations of the model predictions with the actual noise levels can be expected. The comparison and statistical analysis were performed both at a local (per NOMOS station) and a global level (entire NOMOS system).

The agreement with the model improves significantly throughout the years (2012–2018), evolving from an underestimation of the model predictions to a slight overprediction. Specifically, for 2018, the correlation coefficient between measured and modelled $L_{den}$ (for all NOMOS stations) is high and equal to 0.91 and the average difference amounts to only 0.9 dB(A).

The measured $L_{den}$ trend throughout the years was also investigated. Supported by aircraft noise certification data, we have demonstrated qualitatively that the observed decrease in $L_{den}$ of 3.6 dB(A) (for the period 2012–2018) can be explained by the fact

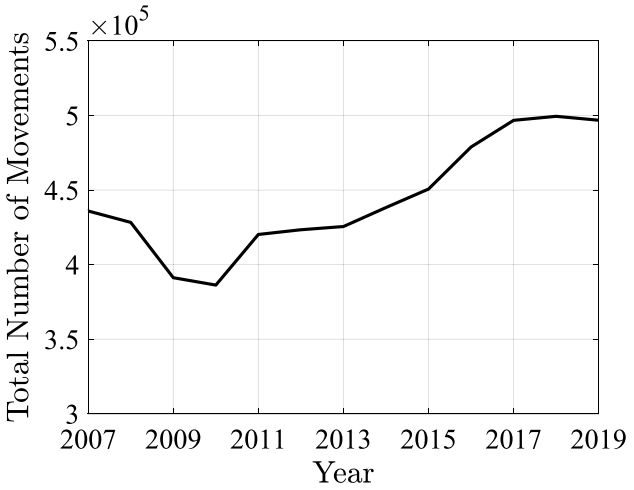


**Fig. 10.** Total number of flight movements (take-offs and landings) per year (including freight) for the period 2007–2019.

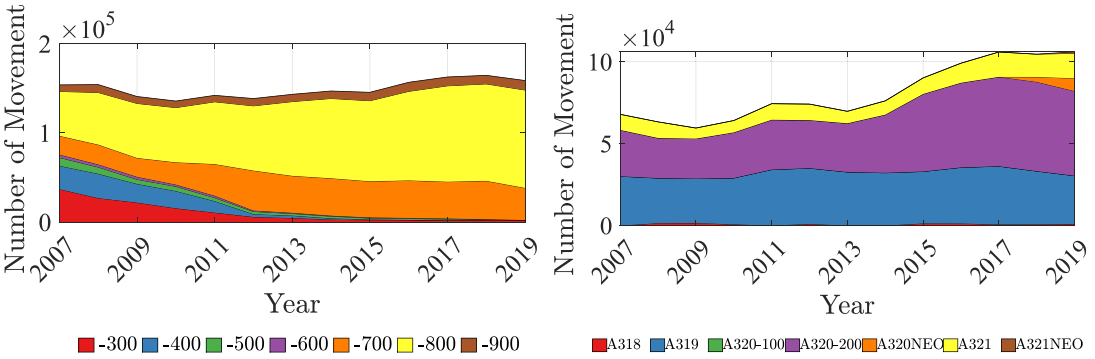


(a) Number of movements between 2007 and 2019 of the B737 family.

(b) Number of movements between 2007 and 2019 of the Airbus family.

(c) Number of movements between 2007 and 2019 of the Embraer and Fokker.

(d) Number of movements between 2007 and 2019 of the Boeing Widebody family.

**Fig. 11.** Number of flight movements per year for the most frequently occurring aircraft types at Schiphol for the period 2007–2019.

that the most frequently occurring aircraft types at Schiphol in 2019 are less noisy than those in 2007. Furthermore, we observed a sudden decrease in the noise levels which coincides with the implementation of the updated Noise Abatement Departure Procedures (NADP-2) in 2014. From the same year on, we also noticed an improvement in the agreement level between measured and modelled values. Hence, the model might perform better with these new types of aircraft.

**Table 4**
Noise certification data.

| Situation 2007 | | | | | Situation 2019 | | | | |
|---|---|---|---|---|---|---|---|---|---|
| Aircraft Type | MTOW (t) | Lateral (EPNdB) | Flyover (EPNdB) | Approach (EPNdB) | Aircraft Type | MTOW (t) | Lateral (EPNdB) | Flyover (EPNdB) | Approach (EPNdB) |
| 737-300 | 61 | 90.5 | 84.4 | 98.6 | 737-700 | 62 | 93.3 | 83.2 | 95.8 |
| 737-400 | 66 | 90.8 | 85.7 | 98.4 | 737-800 | 74 | 93.8 | 85.3 | 96.2 |
| 737-500 | 58 | 89.6 | 83.7 | 97.9 | | | | | |
| 767-300 | 182 | 96.4 | 88.8 | 98.5 | 777-200 | 298 | 96.6 | 90.0 | 99.1 |
| 747-400 | 395 | 98.7 | 97.4 | 103 | 777-300 | 349 | 98.5 | 90.4 | 100.2 |
| | | | | | 787-9 | 253 | 91.8 | 85.9 | 96.1 |
| F70 | 37 | 89.8 | 77.8 | 88.1 | E170 | 38 | 92.0 | 82.5 | 94.7 |
| F100 | 45 | 90.6 | 82.6 | 93.1 | E190 | 45 | 92.3 | 84.3 | 92.6 |
| | | | | | A319 | 66 | 92.3 | 83.1 | 93.7 |
| | | | | | A320 | 75 | 92.6 | 84.4 | 95.3 |
| | | | | | A321 | 87 | 96.1 | 86.7 | 96.5 |

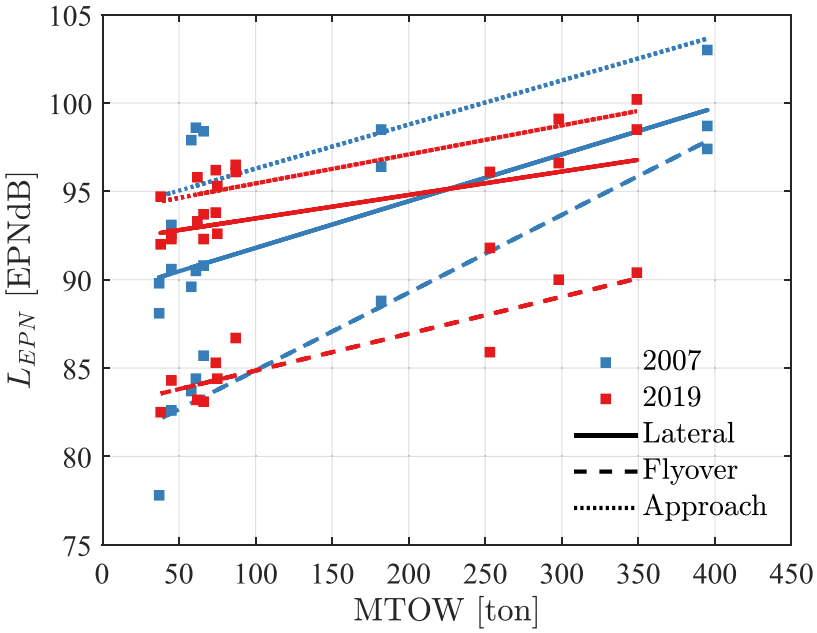


**Fig. 12.** Noise certification data of the most frequently occurring aircraft at Schiphol plotted as a function of their MTOW value. Blue: data for 2007. Red: data for 2019. The data have been linearly least-squares fitted, where a distinction has been made between the 'lateral', 'flyover' and 'approach' data. (For interpretation of the references to colour in this figure legend, the reader is referred to the web version of this article.)

Another observation regards the consistent decrease in $L_{night}$ both for aircraft related events and total noise. This leads us to believe that most of the night-time total noise comes from aircraft. The 3.1 dB(A) decrease throughout the years might be due to both the CDA procedures used during night-time and the higher take-off and landing rates.

This study has shown that improved Noise Abatement Departure Procedures (for take-off) and CDA (for landing) at Schiphol, and changes in fleet mix to less noisy aircraft, lead to less noise exposure for the residents around Schiphol Airport.

Further, the assessment method described in this paper can be used for a noise exposure analysis per runway and for specific operational procedures, which are particularly useful for policy-makers.

## References

Basner, M., McGuire, S., 2018. WHO Environmental noise guidelines: systematic review on environmental noise and effects on sleep. Int. J. Environ. Res. Public Health 15 (3), A156. http://dx.doi.org/10.1093/sleepj/zsx050.420.

Bertsch, L., Simons, D.G., Snellen, M., 2015. Aircraft Noise: The major sources, modelling capabilities, and reduction possibilities. Technical Report DLR-Interner Bericht. DLR-IB 224-2015 A 110, Deutsches Zentrum fur Luft- und Raumfahrt, http://dx.doi.org/10.34912/ac-n0is3, URL https://elib.dlr.de/95939/.

Bewoners Aanspreekpunt Schiphol, 2021. 2020 Jaarrapportage. Technical Report, Bewoners Aanspreekpunt Schiphol, Amsterdam, pp. 1–52, URL www.minderhinderschiphol.nl.

Casper.Aero, 2021. NOMOS Online (NL). URL https://noiselab.casper.aero/ams/#page=n_over_nomos.
Chatfield, C., Bendat, J.S., Piersol, A.G., 1987. Random data: Analysis and measurement procedures. J. R. Stat. Soc. Series A (General) 150 (2), 167. http://dx.doi.org/10.2307/2981634.
Council of the European Union, 2002. Directive 2002/49/EC of the European parliament and of the council - assessment and management of environmental noise. Off. J. Eur. Communities L 189, 12–25, URL http://data.europa.eu/eli/dir/2002/49/oj.
Crocker, M.J., 2008. Fundamentals of acoustics, noise, and vibration. In: Handbook of Noise and Vibration Control. John Wiley & Sons, Ltd, pp. 1–16. http://dx.doi.org/10.1002/9780470209707.
Dobruszkes, F., Efthymiou, M., 2020. When environmental indicators are not neutral: Assessing aircraft noise assessment in Europe. J. Air Transp. Manag. 88 (March), http://dx.doi.org/10.1016/j.jairtraman.2020.101861.
EASA, 2020. EASA Certification noise levels. In: EASA European Union Aviation Safety Agency. URL https://www.easa.europa.eu/domains/environment/easa-certification-noise-levels#group-easa-downloads.
ECAC.CEAC, 2016. Doc 29 4th Edition Volume 2: Technical Guide - Report on Standard Method of Computing Noise Contours around Civil Airports, Vol.2, 4th Ed. (December), p. 139, URL https://www.ecac-ceac.org/images/documents/ECAC-Doc_29_4th_edition_Dec_2016_Volume_2.pdf.
European Aircraft Noise Services, 2021. EANS - European Aircraft noise services - schiphol. URL https://www.eans.net/.
Franssen, E.A.M., van Wiechen, C.M.A.G., Nagelkerke, N.J.D., Lebret, E., 2004. Aircraft noise around a large international airport and its impact on general health and medication use. Occup. Environ. Med. 61 (5), 405–413. http://dx.doi.org/10.1136/oem.2002.005488.
Geng, D., Yi, K., Shang, C., Yang, J., He, Y., 2015. Application status of composite acoustic liner in aero-engine. In: 10th International Conference on Composite Science and Technology.
Gjestland, T., 2019. Aircraft noise annoyance. In: 2019 Environmental Report: Aviation and Environment. Technical Report, pp. 89–92, URL https://www.icao.int/environmental-protection/pages/envrep2019.aspx.
Hansell, A.L., Blangiardo, M., Fortunato, L., Floud, S., de Hoogh, K., Fecht, D., Ghosh, R.E., Laszlo, H.E., Pearson, C., Beale, L., Beevers, S., Gulliver, J., Best, N., Richardson, S., Elliott, P., 2013. Aircraft noise and cardiovascular disease near heathrow airport in London: Small area study. BMJ (Online) 347 (7928), http://dx.doi.org/10.1136/bmj.f5432.
Heppe, G.J.T., 2014. Appendices van de voorschriften voor de berekening van de geluidsbelasting in Lden en Lnight voor Schiphol. Technical Report NLR-CR-96650L, Nationaal Lucht-en Ruimtevaartlaboratorium, Amsterdam.
Merino-Martínez, R., Heblij, S.J., Bergmans, D.H.T., Snellen, M., Simons, D.G., 2018. Improving aircraft noise predictions considering fan rotational speed. J. Aircr. 56 (1), 284–294. http://dx.doi.org/10.2514/1.C034849.
Merino-Martínez, R., Snellen, M., Simons, D.G., 2016a. Functional beamforming applied to imaging of flyover noise on landing aircraft. J. Aircr. 53 (6), 1830–1843. http://dx.doi.org/10.2514/1.C033691.
Merino-Martínez, R., Snellen, M., Simons, D.G., Bertsch, L., 2016b. Analysis of landing gear noise during approach. In: 22nd AIAA/CEAS Aeroacoustics Conference, 2016. http://dx.doi.org/10.2514/6.2016-2769.
Ministerie van Infrastructuur en Milieu, 2014. Tijdelijke vrijstelling van artikel 23 van de Regeling luchtverkeersdienstverlening in verband met de uitvoering van de NADP2 procedure. De Staatssecretaris van Infrastructuur en Milieu, pp. 1–2, URL https://zoek.officielebekendmakingen.nl/stcrt-2014-11802.html.
Morrell, P., Lu, C.H.Y., 2000. Aircraft noise social cost and charge mechanisms - a case study of amsterdam airport schiphol. Transp. Res. Part D: Transp. Environ. 5 (4), 305–320. http://dx.doi.org/10.1016/S1361-9209(99)00035-8.
Schiphol Airport, 2021. Schiphol | AMS airport charges, levies, slots and conditions. URL https://www.schiphol.nl/nl/route-development/pagina/ams-airport-charges-levies-slots-and-conditions/.
Sijtsma, P., 2010. Phased array beamforming applied to wind tunnel and fly-over tests. SAE Tech. Pap. (October), 22. http://dx.doi.org/10.4271/2010-36-0514.
Siller, H.A., 2012. Localisation of sound sources on aircraft in flight. In: American Society of Mechanical Engineers, Noise Control and Acoustics Division (Publication) NCAD. pp. 193–202. http://dx.doi.org/10.1115/NCAD2012-0575.
Simons, D.G., Snellen, M., van Midden, B., Arntzen, M., Bergmans, D.H.T., 2015. Assessment of noise level variations of aircraft flyovers using acoustic arrays. J. Aircr. 52 (5), 1625–1633. http://dx.doi.org/10.2514/1.C033020.
Snellen, M., Merino-Martínez, R., Simons, D.G., 2017. Assessment of noise variability of landing aircraft using phased microphone array. J. Aircr. 54 (6), 2173–2183. http://dx.doi.org/10.2514/1.C033950.
Strategische Milieuverkenning, 2008. Kaartbijlage voor de ontwikkeling van Schiphol op middellange termijn: Bijlage A - Gebruik INM voor analyse 2020-situaties. Technical Report, Schiphol Group; Luchtverkeersleiding Nederland, p. 108, URL https://www.omgevingsraadschiphol.nl/wp-content/uploads/2015/08/20081024_strategische-milieuverkenning-schiphol.pdf.
Veerbeek, H.W., Brouwer, M.A., 2012. Noise measurement analysis during a noise abatement departure procedure trial. 41st Int. Cong. Expo. Noise Control Eng. 2012, INTER-NOISE 2012 7, 5408–5418.
Vieira, A., Snellen, M., Simons, D.G., 2020. Experimental assessment of sound quality metrics for takeoff and landing aircraft. AIAA J. 59 (1), 240–249. http://dx.doi.org/10.2514/1.J059633.
van der Wal, H.M.M., Vogel, P., Wubben, F.J.M., 2001a. Voorschrift voor de berekening van de Lden en Lnight geluidbelasting in dB(A) ten gevolge van vliegverkeer van en naar de luchthaven Schiphol. Part 1: Berekeningsvoorschrift,Vol. 1. Technical Report NLR-CR-2001-372-PT-1, Nationaal Lucht-en Ruimtevaartlaboratorium, Amsterdam.
van der Wal, H.M.M., Vogel, P., Wubben, F.J.M., 2001b. Voorschrift voor de berekening van de Lden en Lnight geluidbelasting in dB(A) ten gevolge van vliegverkeer van en naar de luchthaven Schiphol. Part 2: Toelichting op het berekeningsvoorschrift, Vol. 2. Technical Report NLR-CR-2001-372-PT-2, Nationaal Lucht-en Ruimtevaartlaboratorium, Amsterdam.
WorldPop and Center for International Earth Science Information Network (CIESIN), 2020. The spatial distribution of population density in 2019, netherlands. http://dx.doi.org/10.5258/SOTON/WP00674, URL https://www.worldpop.org/geodata/summary?id=42732.
Zellmann, C., Schäffer, B., Wunderli, J.M., Isermann, U., Paschereit, C.O., 2017. Aircraft noise emission model accounting for aircraft flight parameters. J. Aircr. 55 (2), 682–695. http://dx.doi.org/10.2514/1.C034275.